IEEE Access
Multidisciplinary ⋮ Rapid Review ⋮ Open Access Journal

Received 17 December 2022, accepted 15 January 2023, date of publication 18 January 2023, date of current version 24 January 2023.

Digital Object Identifier 10.1109/ACCESS.2023.3237853

RESEARCH ARTICLE

Computational Method for Specific Energy Loss by Fast Inverse Laplace Transform

SEIYA KISHIMOTO, (Member, IEEE), AND SHINICHIRO OHNUKI, (Member, IEEE)
College of Science and Technology, Nihon University, Tokyo 101-8308, Japan

Corresponding author: Seiya Kishimoto (kishimoto.seiya@nihon-u.ac.jp)

This work was supported in part by Japan Society for the Promotion of Science (JSPS) KAKENHI under Grant JP21K17753, and in part by the Research Grant from the College of Science and Technology, Nihon University.

ABSTRACT This study proposes a novel computational technique for specific energy loss for pulse incidence. Our method is based on a fast inverse Laplace transform (FILT) with an electromagnetic field solver in the complex frequency domain. Using the FILT algorithm, the specific energy loss in the complex frequency domain can be computed and transformed into the time domain. In our method, the specific energy loss can be computed until the desired observation time without solving the electromagnetic field at the previous observation time. The finite-difference complex-frequency domain (FDCFD) was used for the complex frequency domain solver. The results demonstrated that our proposed method could compute the dissipated energy of inhomogeneous, non-dispersive lossy dielectrics.

INDEX TERMS Complex frequency domain, convolution integral, fast inverse Laplace transform, specific energy, time-domain solver.

I. INTRODUCTION

Pulse incidence requires analysis of specific energy absorbed in biological medium. Conventionally, energy is computed using electromagnetic fields updated by time-domain solvers, such as the finite-difference time-domain (FDTD) method [1], [2]. Sequential computation is commonly used to calculate specific energy, as shown in Fig. 1. In the conventional method, the specific energy is calculated from the time response of fields obtained using time-domain solvers and is integrated. To evaluate the specific energy in the case of pulse incidence, sequential computations must be performed until the time response of the field becomes sufficiently small. For efficient computation, a computational method that can evaluate the specific energy without obtaining the time response is required.

A novel computational technique based on fast inverse Laplace transform (FILT) is proposed for evaluating the specific energy loss caused by an impinging pulse. FILT is used as a solver for transient electromagnetic problems [3], [4], [5], [6], [7], [8]. In the proposed method, it is directly computed without the time response of fields. This is useful for calculating specific energy loss after pulse-wave irradiation because time response of specific energy is evaluated using a large time-step size and without evaluating the time evolution or updating the field in space. The advantages of the proposed method are that the solution can be computed at a specific observation time, sequential computation is not required, and high parallel efficiency is obtained. The objective medium is assumed to be a non-dispersive lossy medium. Furthermore, we recently developed time-division parallel computing for reducing the computational time of FDTD, which is referred to as the conventional method in this paper [9], [10], [11]. The proposed direct computational method is required to evaluate specific energy loss in time-division parallel computation and can contribute to speeding up the conventional FDTD.

FILT is a numerical method for computing the inverse Laplace transform, and it computes the transient response with controlled accuracy. Compared with other numerical inverse Laplace transform methods, this algorithm determines the sampling points in the complex frequency domain [12], [13], [14], [15], [16], [17], [18], [19]. By utilizing the Euler transformation, it is possible to reduce the number of calculations. In addition, it can independently calculate electromagnetic fields at arbitrary times and is suitable for

The associate editor coordinating the review of this manuscript and approving it for publication was Debdeep Sarkar.

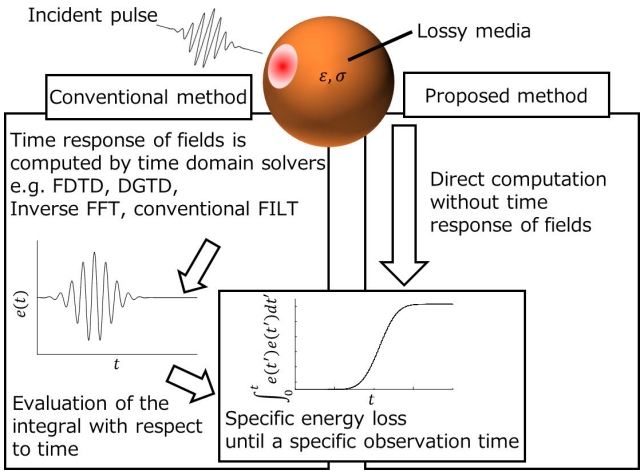

FIGURE 1. Computation method for the specific energy loss until an observation time. In the conventional method, it is calculated from the time response of fields obtained using time-domain solvers and is integrated. In the proposed method, it is directly computed, without the time response of fields.

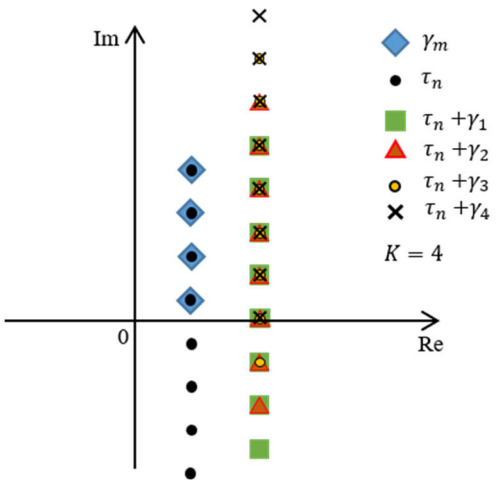

FIGURE 2. The complex plane and poles for FILT and evaluation of the convolutional integral. These poles indicate the sampling frequency.

parallel computation [9], [10], [11]. However, the computation of the specific energy up until the observation time using FILT has not been investigated. Hence, the time response of the electric field or the evaluation of the convolution integral in the complex frequency domain is required. In this study, the specific energy loss until the observation time was obtained by adding the function values in the complex frequency domain.

The remainder of this paper is organized as follows. Section II presents a direct computation method for the specific energy loss using FILT. The computational results are described in Section III. The paper ends with a conclusion in Section IV.

II. FORMULATION

A. SPECIFIC ENERGY LOSS

The specific energy loss SA_{Lt} for lossy media until observation time t is given by the following equation [1]:

$$SA_{Lt}(t) = \frac{\sigma}{\rho}\int_0^t \boldsymbol{e}(t')\cdot\boldsymbol{e}(t')\,dt', \tag{1}$$

where ρ is the mass density of the medium, σ is the conductivity, and e is the electric field in the time domain.

Considering the Laplace transform of (1), the specific energy loss in the complex frequency domain SA_{Ls} is expressed as [20], [21], and [22]

$$SA_{Ls}(s) = \frac{\sigma}{\rho}\boldsymbol{E}*\boldsymbol{E}(s), \tag{2}$$

where s is the complex frequency and E is the electric field in the complex frequency domain.

$$\boldsymbol{E}*\boldsymbol{E}(s) = \frac{1}{2\pi i}\int_{c-i\infty}^{c+i\infty}\boldsymbol{E}(\gamma)\cdot\boldsymbol{e}(s-\gamma)\,d\gamma, \tag{3}$$

where γ is the complex frequency, and c is a real number such that the contour path of integration is in the region of convergence of $\boldsymbol{E}(\gamma)$.

B. INVERSE LAPLACE TRANSFORM FOR SPECIFIC ENERGY LOSS IN COMPLEX FREQUENCY DOMAIN

In this section, $f(t)$ and $g(t)$ are considered as functions in the time domain. $F(s)$ and $G(s)$ are considered as functions in the complex frequency domain. In the FILT, the time-domain function $f(t)$ is numerically computed using the complex frequency domain function $F(s)$ as follows:

$$f(t) \approx \frac{e^{\alpha}}{t}\sum_{n=1}^{K}(-1)^n \operatorname{Im}\left[F(s_n)\right]. \tag{4}$$

Here,

$$s_n = \frac{\alpha + i(n-0.5)\pi}{t}, \tag{5}$$

where α is the approximation parameter, and K is the truncation number.

The integration of $f(t)g(t)$ in the time domain is expressed as the product of $1/s$ and the convolution integral $F*G(s)$ in the complex frequency domain.

$$L\left[\int_0^t f(t')\,g(t')\,dt'\right] = \frac{1}{s}F*G(s) = H(s)F*G(s), \tag{6}$$

where $H(s)$ denotes the image function. The convolution integral is computed to transform (6) into the time domain. Using the FILT, the time-domain function is expressed as

$$L^{-1}\left[H(s)\,F*G(s)\right] \approx \frac{e^{\alpha}}{t}\sum_{m=1}^{K}(-1)^m \operatorname{Im}\left[F(\gamma_m)\,I(\gamma_m)\right], \tag{7}$$

where

$$\gamma_m = \frac{\alpha + i(m-0.5)\pi}{t} \tag{8}$$

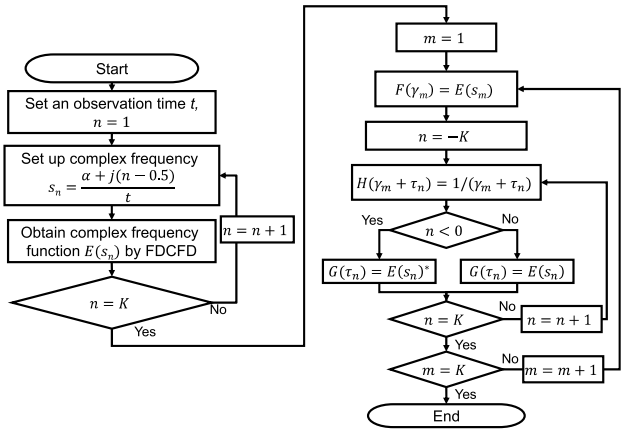

FIGURE 3. Flowchart for computing the specific energy loss until the observation time t using our method.

$$I(\gamma_m) \approx \frac{ie^{\alpha}}{2t} \sum_{n=-K}^{K} (-1)^{n+1} H(\tau_n + \gamma_m) G(\tau_n) \quad (9)$$

$$\tau_n = \frac{\alpha + i(n-0.5)\pi}{t}. \quad (10)$$

Using (7), the specific energy loss SA_{Lt} until the observation time t can be directly computed. Image functions $F(\gamma_m)$, $G(\tau_n)$ and $H(\tau_n + \gamma_m)$ are required for computing (7). γ_m and τ_n are poles in the complex frequency domain, indicating the sampling frequency. The distribution of poles is shown in Fig. 2 when the infinite series was truncated considering $K = 4$. γ_m changes from 1 to K, and τ_n changes from $-K$ to K.

C. COMPUTATIONAL FLOW FOR PROPOSED METHOD

Fig. 3 shows a flowchart for computing the specific energy loss SA_{Lt} using (7). The inverse Laplace transform of complex frequency-domain functions, including a convolution integral and integral with respect to time, can be expressed as a series. First, for the sampling frequency determined by FILT, the electric field in the complex frequency domain $E(s_n)$ is obtained using the complex-frequency-domain solver. In this study, it is calculated using finite-difference complex-frequency domain (FDCFD) [7]. Then, (7) is computed. Here, $F(\gamma_m)$ and $G(\tau_n)$ are calculated by substituting $E(s_n)$.

III. COMPUTATIONAL RESULTS

To verify the proposed method, it was established that the time response of the energy could be obtained without the time response of the electric field. The time response of the energy was analyzed for electromagnetic-wave propagation in air, as shown in Fig. 4. The source was assumed to be a sinusoidal continuous plane wave at 2.4 GHz. The observation point was located at the center of the analysis area and at the same position as that of the source.

Fig. 5 depicts the time response of the total power with respect to the observation time. The solid line indicates that the exact solution can be obtained using $e_y(t) = \sin \omega t$. The dashed line represents the FDTD results derived from the

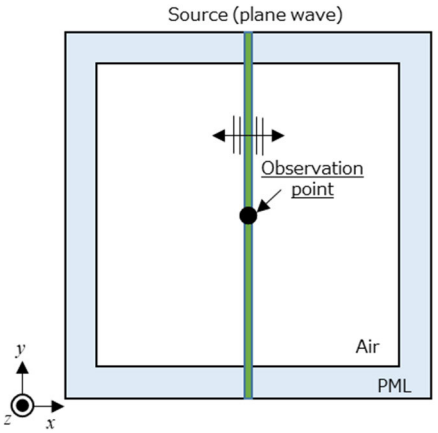

FIGURE 4. Geometry for validating that energy can be obtained without the time response of the electric field.

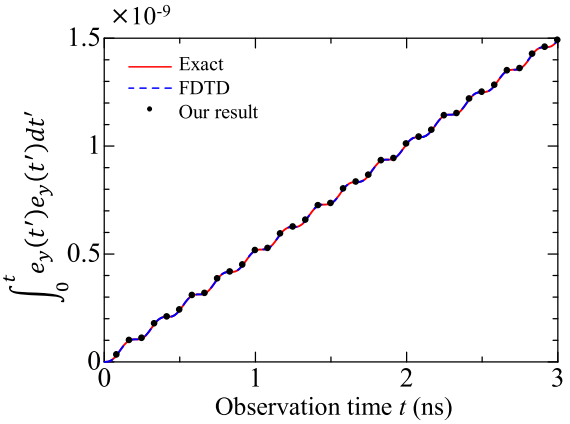

FIGURE 5. Time response of total power density for plane wave propagation.

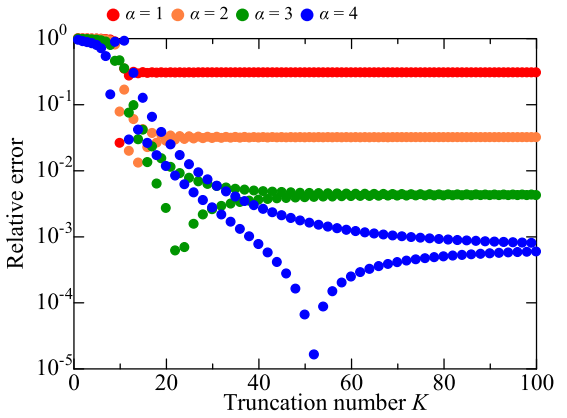

FIGURE 6. Convergence process for varying the truncation number K. The relative error is computed using the exact value, and the result is at $t = 2$ ns.

sequential calculation. Dots denote the results of this study. All the results were in good agreement.

To validate the computational accuracy of our method, Fig. 6 shows the convergence process of the relative error for varying truncation number K of FILT. The relative error is defined by the exact solution and our results with an observation time of $t = 2$ ns. The relative error decreases by increasing the truncation number K. Furthermore, the approximation parameter α and the digits of the convergence

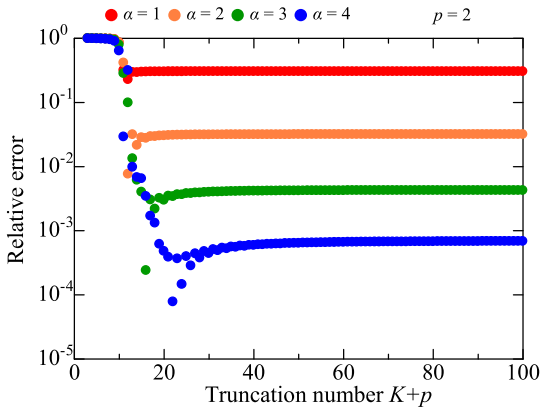

FIGURE 7. Convergence process for varying the truncation number K with Euler transformation. The order for Euler transformation is $p = 2$.

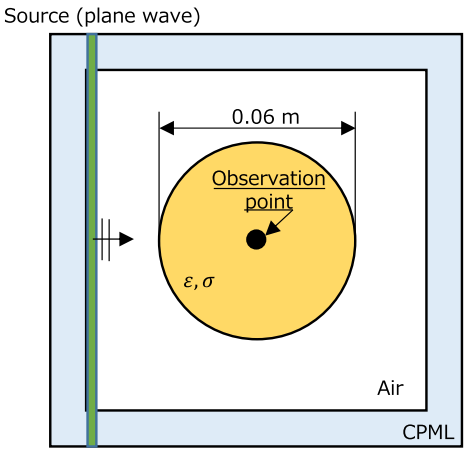

FIGURE 8. Computational model for the demonstration of our method. The scatterer consists of a lossy dielectric with permittivity $\varepsilon = \varepsilon_r \varepsilon_0$ and conductivity σ.

value agree. However, when $\alpha = 4$, sufficient convergence cannot be confirmed, even if $K > 100$.

FILT is a powerful algorithm for transient analyses and computation of instantaneous values. However, the number of terms in (7) increases, such as the computation of an instantaneous value with a large observation time. Euler transformation is applied to the two series of (7) to obtain the rapid convergence of the specific energy loss computation.

$$L^{-1}\left[H(s)F * G(s)\right] \approx \frac{e^{\alpha}}{t}\left(\sum_{m=1}^{K}(-1)^m \operatorname{Im}\left[F(\gamma_m) I(\gamma_m)\right] + \sum_{q=0}^{p-1} A_{pq}(-1)^{K+1+q} \operatorname{Im}\left[F\left(\gamma_{K+1+q}\right) I\left(\gamma_{K+1+q}\right)\right]\right). \tag{11}$$

Here,

$$I(\gamma_m) = \frac{ie^{\alpha}}{2t}\left[\sum_{n=-K}^{K}(-1)^{n+1} H(\tau_n + \gamma_m) G(\gamma_m) + \sum_{q=0}^{p-1} A_{pq}\left((-1)^{n+1} H\left(\tau_{K+1+q} + \gamma_m\right) \times G\left(\gamma_{K+1+q}\right) + (-1)^{n+1} H\left(\tau_{-K-1-q} + \gamma_m\right) \times G\left(\gamma_{-K-1-q}\right)\right)\right]$$

$$A_{pq} = 2^{-p}\sum_{k=0}^{p-q-1} C_{mn}(p,k),$$

where $C_{mn}(p,k)$ is the binomial coefficient.

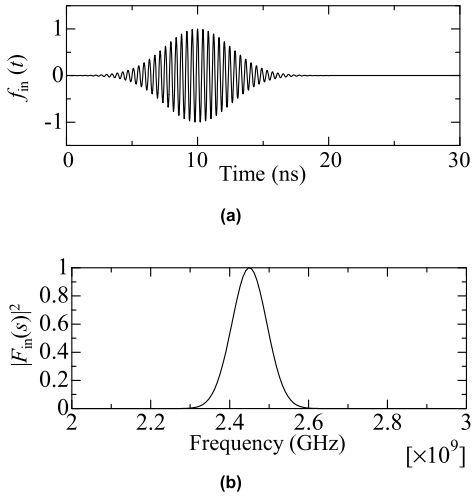

FIGURE 9. Incident waveform in the time and frequency domain. The modulated gaussian pulse with center frequency $f_c = 2.45$ GHz is assumed. (a) Time domain and (b) frequency domain.

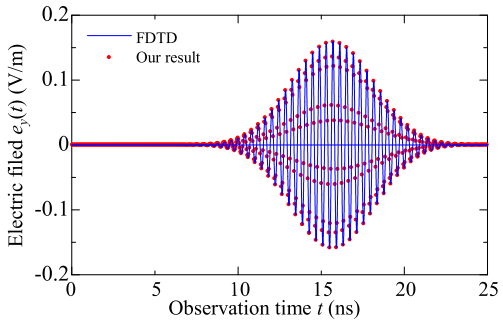

FIGURE 10. Time domain response of electric field at the observation point. Our results and FDTD results are in good agreement.

Fig. 7 shows the convergence process with the Euler transformation. The order of the Euler transformation was $p = 2$. Fast convergence can be achieved with all the error parameters. In particular, when $\alpha = 4$, sufficient convergence can be confirmed with $K > 50$.

To demonstrate our proposed method, electromagnetic scattering problems for a lossy dielectric cylinder were solved. The computational model is shown in Fig. 8. The medium is muscle. Relative permittivity $\varepsilon_r = 52.729$ and conductivity $\sigma = 1.7388$ with a frequency of 2.45 GHz were used [23]. A cylinder with a radius of 3 cm was modeled using a staircase approximation. The same space step sizes (0.03/50 m) for Δx and Δy are used. The absorbing boundary condition is assumed to be a convolutional perfectly matched

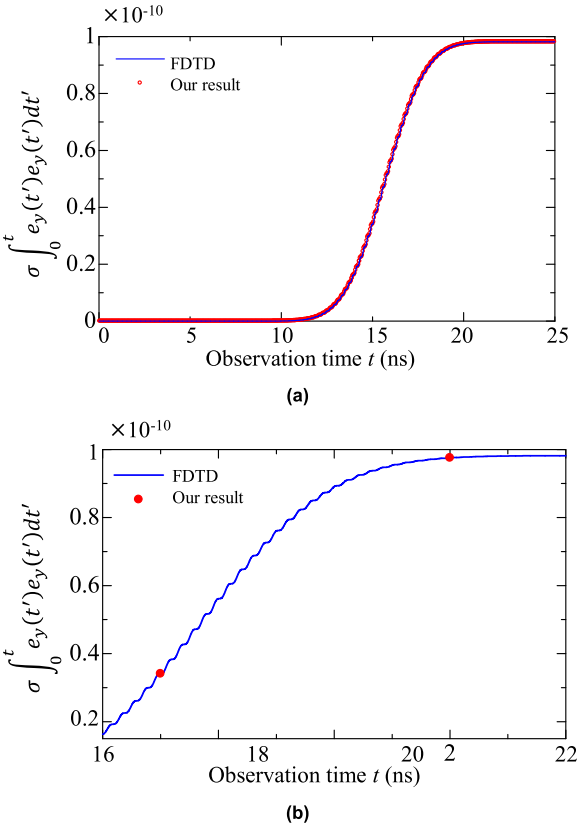

FIGURE 11. Time-domain response of electric energy at the observation point. Our method can compute the electric energy until the observation time. (a) Overall observation time and (b) enlarged view with our result of calculating only $t = 15$ ns and 20 ns.

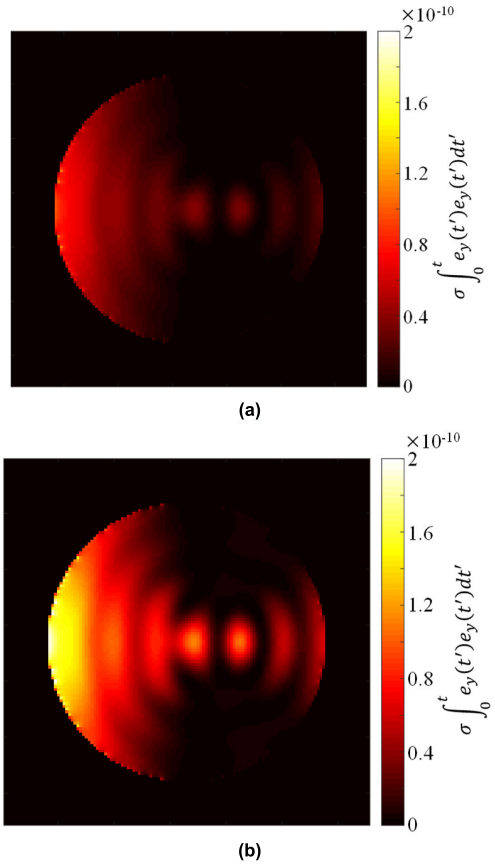

FIGURE 12. Field distribution of the electric energy until the observation time. Our method can calculate the field distribution for a specified observation time. (a) $t = 15$ ns and (b) $t = 20$ ns.

layer (CPML). The incident wave is a linearly polarized wave in which the electric field has only a y-component.

Figs. 9(a) and (b) show the incident waveforms in the time and frequency domains, respectively. A modulated Gaussian pulse with center frequency $f_c = 2.45$ GHz is assumed.

To obtain the dissipated energy up until the observation time using (11), FDCFD was used for the complex frequency domain solver [7]. Fig. 10 shows the time response of the electric field at the observation point to verify that FDCFD-FILT can obtain the time-domain response. The electric field in the time and complex frequency domains can be accurately computed owing to the consistency of all the results.

Fig. 11(a) shows the electric energy dissipated until the observation time. Our results were derived from a previous study [18]. Here, $F(\gamma_m)$ is the electric field in the complex frequency domain, which was obtained using FDCFD. The time-step size of the FDCFD-FILT is not restricted and is set to one-tenth of one cycle for 2.45 GHz. Compared to the FDTD results, our results can compute the time response of the electric energy for all observation times. Fig. 11(b) shows an enlarged view of Fig. 11(a). Our method can compute the electric energy up to a specific observation time without the time response of the electric field. Hence, the energy can be selectively computed until the specific observation times t = 15 ns and 20 ns.

TABLE 1. Comparison of CPU time.

Number of Nodes	CPU time (s)	
	Proposed method	FDTD
1	2508	2821
2	1256	-
5	510	-
10	253	-

Figs. 12(a) and (b) show the dissipated electric-energy field distributions for $t = 15$ and 20 ns, respectively. When the time response of the energy at the observation point is computed, as shown in Fig. 11, the electric field in the complex-frequency region of the entire analysis region is calculated by FDCFD. Using the FILT, the field distribution can be calculated for a specified observation time.

Finally, the computation times were compared. Table 1 lists the CPU times of the proposed method and FDTD. The specific absorption loss was computed at an observation time of $t = 30$ ns. The proposed method is faster than the FDTD method; thus, it is suitable for parallel computing. The complex frequency function $F(s_n)$ was solved and computed using multiple computers. Furthermore, the specific absorption loss calculation using the proposed method is also important for the parallel computation of time-division parallel FDTD, which we recently developed [9], [10], [11].

IV. CONCLUSION

A computational method for time-domain electromagnetic energy was proposed in this study. At a specific observation time, the electromagnetic energy was directly computed without the time response of the electric field. We used the standard FDCFD, demonstrating that the dissipated energy of inhomogeneous, non-dispersive lossy dielectrics can be computed. Therefore, it is necessary to apply a dispersible medium in future studies. The results indicated that the computational time can be reduced by changing the method based on the wave equation.

APPENDIX A
FAST INVERSE LAPLACE TRANSFORM

To obtain time-domain solutions, the complex frequency-domain function is transformed using FILT. Our algorithm accurately obtains the instantaneous value at a single moment, and the sampling complex frequency can be directly determined from the algorithm.

The inverse Laplace transform is defined as Bromwich integral [20], [21], [22] as follows:

$$f(t) = \frac{1}{2\pi i}\int_{l-i\infty}^{l+i\infty} F(s)\, e^{st} ds, \tag{A1}$$

where t is the time and $F(s)$ is the image function of the original time-domain function $f(t)$. To perform a numerical calculation of the Bromwich integral, the cosine in the hyperbolic function was applied to the exponential function for approximation [3].

$$e^{st} \approx \frac{e^{\alpha}}{2\cosh(st-\alpha)}. \tag{A2}$$

Here, α is the approximation parameter.

Equation (A2) can be expanded in the following series expansion:

$$\frac{e^{\alpha}}{2\cosh(st-\alpha)} = \frac{e^{\alpha}}{2}\sum_{k=-\infty}^{\infty}\frac{(-1)^k}{st-[\alpha+i(k-0.5)\pi]} \tag{A3}$$

for Re$s < \alpha$. The singular points of (A3) can be easily computed as

$$s_n = \frac{\alpha + i(n-0.5)\pi}{t}, \quad n = 0, \pm1, \pm2, \cdots \tag{A4}$$

By substituting (A3) and (A4) into the Bromwich integral and using the residue theorem, the approximated time-domain function $f_{ap}(t,\alpha)$ can be evaluated using the following equation:

$$f_{ap}(t,\alpha) = \frac{ie^{\alpha}}{2t}\sum_{n=-\infty}^{\infty}(-1)^{n+1} F(s_n). \tag{A5}$$

Conventionally, FILT is performed under the following conditions:

1. The image function $F(s)$ is defined and is regular in the right half of the s-plane (Re[s] > 0).
2. $\lim_{s\to\infty} F(s) = 0$.
3. $F(s)^* = F(s^*)$.

Using Condition 3, the number of terms in (A5) can be reduced by half. The final form of FILT can be obtained by truncating the infinite series as (4).

APPENDIX B
FORMULATION FOR EQUATION (7)

Using the Bromwich integral, the product of the image function and convolution integral is transformed into the time domain as follows:

$$\begin{aligned}
&L^{-1}[H(s)F*G(s)] \\
&= \frac{1}{2\pi i}\int_{l-i\infty}^{l+i\infty} H(s)\, F*G(s)\, e^{st} ds \\
&= \frac{1}{2\pi i}\int_{l-i\infty}^{l+i\infty} H(s)\frac{1}{2\pi i}\int_{c-i\infty}^{c+i\infty} F(\gamma)\, G(s-\gamma)\, d\gamma e^{st} ds
\end{aligned}$$

Using $\exp(st) = \exp((s-\gamma)t)\exp(\gamma t)$ and $s - \gamma = \tau$,

$$\begin{aligned}
&L^{-1}[H(s)F*G(s)] \\
&= \frac{1}{2\pi i}\int_{l-i\infty}^{l+i\infty} H(s)\frac{1}{2\pi i}\int_{c-i\infty}^{c+i\infty} F(\gamma)\, G(s-\gamma)\, e^{(s-\gamma)t} e^{\rho t} d\gamma ds \\
&= \frac{1}{2\pi i}\int_{l-i\infty}^{l+i\infty} F(\gamma)\frac{1}{2\pi i}\int_{c-i\infty}^{c+i\infty} H(s)\, G(s-\gamma)\, e^{(s-\gamma)t} ds e^{\gamma t} d\gamma \\
&= \frac{1}{2\pi i}\int_{l-i\infty}^{l+i\infty} F(\gamma)\frac{1}{2\pi i}\int_{c-i\infty}^{c+i\infty} H(\tau+\gamma)\, G(\tau)\, e^{\tau t} d\tau e^{\gamma t} d\gamma.
\end{aligned}$$

Because the integral with respect to τ is in the Bromwich integral form, it can be applied to the FILT algorithm. Here, $H(\tau+\gamma)^* \neq H(\tau^*+\gamma)$ was considered. The integral with respect to τ can be expressed in a series form as

$$\begin{aligned}
I(\gamma) &= \frac{1}{2\pi i}\int_{c-i\infty}^{c+i\infty} H(\tau+\gamma)\, G(\tau)\, e^{\tau t} d\tau \\
&\approx \frac{ie^{\alpha}}{2t}\sum_{n=-K}^{K}(-1)^{n+1} H(\tau_n+\gamma)\, G(\tau_n),
\end{aligned} \tag{B1}$$

where

$$\tau_n = \frac{\alpha + i(n-0.5)\pi}{t}.$$

The integral with respect to ρ can be computed using the conventional FILT algorithm. Finally, $L^{-1}[H(s)F*G(s)]$, which includes the convolution integral, can be expanded to a series formula as follows:

$$L^{-1}[H(s)F*G(s)] = \frac{1}{2\pi i}\int_{l-i\infty}^{l+i\infty} F(\gamma)\, I_n(\gamma)\, e^{\gamma t} d\gamma$$

$$\approx \frac{e^{\alpha}}{t} \sum_{m=1}^{\infty} \left[(-1)^m \operatorname{Im} \left[F\left(\gamma_m\right) I\left(\gamma_m\right) \right] \right]$$
$$\approx \frac{e^{\alpha}}{t} \sum_{m=1}^{K} F_m, \tag{B2}$$

where

$$\gamma_m = \frac{\alpha + i\left(m - 0.5\right)\pi}{t}$$
$$F_m = (-1)^m \operatorname{Im} \left[F\left(\gamma_m\right) I\left(\gamma_m\right) \right].$$

REFERENCES

[1] J. Chakarothai, S. Watanabe, and K. Wake, "Numerical dosimetry of electromagnetic pulse exposures using FDTD method," *IEEE Trans. Antennas Propag.*, vol. 66, no. 10, pp. 5397–5408, Oct. 2018, doi: 10.1109/TAP.2018.2862344.

[2] A. Taflove and S. C. Hagness, *Computational Electrodynamics*, 2nd ed. Norwood, MA, USA: Artech House, 1995.

[3] T. Hosono, "Numerical inversion of Laplace transform and some applications to wave optics," *Radio Sci.*, vol. 16, no. 6, pp. 1015–1019, Nov./Dec. 1981, doi: 10.1029/RS016i006p01015.

[4] S. Masuda, S. Kishimoto, and S. Ohnuki, "Reference solutions for time domain electromagnetic solvers," *IEEE Access*, vol. 8, pp. 44318–44324, 2020, doi: 10.1109/ACCESS.2020.2977382.

[5] S. Kishimoto, T. Okada, S. Ohnuki, Y. Ashizawa, and K. Nakagawa, "Efficient analysis of electromagnetic fields for designing nanoscale antennas by using a boundary integral equation method with fast inverse Laplace transform," *Prog. Electromagn. Res.*, vol. 146, pp. 155–165, 2014, doi: 10.2528/PIER13081701.

[6] S. Kishimoto, S. Y. Huang, Y. Ashizawa, K. Nakagawa, S. Ohnuki, and W. C. Chew, "Transient analysis method for plasmonic devices by PMCHWT with fast inverse Laplace transform," *IEEE Antennas Wireless Propag. Lett.*, vol. 21, no. 5, pp. 973–977, May 2022, doi: 10.1109/LAWP.2022.3153650.

[7] D. Wu, R. Ohnishi, R. Uemura, T. Yamaguchi, and S. Ohnuki, "Finite-difference complex-frequency-domain method for optical and plasmonic analyses," *IEEE Photon. Technol. Lett.*, vol. 30, no. 11, pp. 1024–1027, Jun. 1, 2018, doi: 10.1109/LPT.2018.2828167.

[8] S. Kishimoto, S. Nishino, and S. Ohnuki, "Novel computational technique for time-dependent heat transfer analysis using fast inverse Laplace transform," *Prog. Electromagn. Res. M*, vol. 99, pp. 45–55, 2021, doi: 10.2528/PIERM20100203.

[9] S. Ohnuki, R. Ohnishi, D. Wu, and T. Yamaguchi, "Time-division parallel FDTD algorithm," *IEEE Photon. Technol. Lett.*, vol. 30, no. 24, pp. 2143–2146, Dec. 15, 2018, doi: 10.1109/LPT.2018.2879365.

[10] D. Wu, S. Kishimoto, and S. Ohnuki, "Optimal parallel algorithm of fast inverse Laplace transform for electromagnetic analysis," *IEEE Antennas Wireless Propag. Lett.*, vol. 19, no. 12, pp. 2018–2022, Dec. 2020, doi: 10.1109/LAWP.2020.3020327.

[11] T. Nakazawa, D. Wu, S. Kishimoto, J. Shibayama, J. Yamauchi, and S. Ohnuki, "Error-controllable scheme for the LOD-FDTD method," *IEEE J. Multiscale Multiphys. Comput. Techn.*, vol. 7, pp. 135–141, 2022, doi: 10.1109/JMMCT.2022.3181568.

[12] K. L. Kuhlman, "Review of inverse Laplace transform algorithms for Laplace-space numerical approaches," *Numer. Algorithms*, vol. 63, no. 2, pp. 339–355, 2013, doi: 10.1007/s11075-012-9625-3.

[13] B. Davies and B. Martin, "Numerical inversion of the Laplace transform: A survey and comparison of methods," *J. Comput. Phys.*, vol. 33, no. 1, pp. 1–32, 1979, doi: 10.1016/0021-9991(79)90025-1.

[14] Q. Wang and H. Zhan, "On different numerical inverse Laplace methods for solute transport problems," *Adv. Water Resour.*, vol. 75, pp. 80–92, Jan. 2015, doi: 10.1016/j.advwatres.2014.11.001.

[15] B. Dingfelder and J. A. C. Weideman, "An improved Talbot method for numerical Laplace transform inversion," *Numer. Algorithms*, vol. 68, no. 1, pp. 167–183, Jan. 2015, doi: 10.1007/s11075-014-9895-z.

[16] F. Loreto, D. Romano, M. Stumpf, A. E. Ruehli, and G. Antonini, "Time-domain computation of full-wave partial inductances based on the modified numerical inversion of Laplace transform method," *IEEE Trans. Signal Power Integrity*, vol. 1, pp. 32–42, 2022, doi: 10.1109/TSIPI.2022.3179250.

[17] B. S. Garbow, G. Giunta, J. N. Lyness, and A. Murli, "Software for an implementation of Weeks' method for the inverse Laplace transform," *ACM Trans. Math. Softw.*, vol. 14, no. 2, pp. 163–170, Jun. 1988, doi: 10.1145/45054.45057.

[18] A. Ahmad, P. Johannet, and Ph. Auriol, "Efficient inverse Laplace transform algorithm for transient overvoltage calculation," *IEE Proc. C, Gener., Transmiss. Distrib.*, vol. 139, no. 2, pp. 117–121, Mar. 1992, doi: 10.1049/ip-c.1992.0019.

[19] X. Liu, M. Zhang, P. Wang, and S. Niu, "A method for the evaluation of Cooray–Rubinstein formula based on Talbot's method for numerical inverse Laplace transform," *IEEE Trans. Electromagn. Compat.*, vol. 61, no. 3, pp. 759–765, Jun. 2019, doi: 10.1109/TEMC.2019.2914177.

[20] D. V. Widder, *The Laplace Transform Princeton Mathematical Series*. Princeton, NJ, USA: Princeton Univ. Press, 1941.

[21] F. Oberhettinger and L. Badii, *Tables of Laplace transform*. Berlin, Germany: Spinger-Verlag, 1973.

[22] M. Abramowitz and I. Stegun, *Handbook of Mathematical Functions with Formulas, Graphs, and Mathematical Table*. New York, NY, USA: Dover, 1964.

[23] S. Gabriel, R. W. Lau, and C. Gabriel, "The dielectric properties of biological tissues: III. Parametric models for the dielectric spectrum of tissues," *Phys. Med. Biol.*, vol. 41, no. 11, pp. 2271–2293, Apr. 1996, doi: 10.1088/0031-9155/41/11/003.

SEIYA KISHIMOTO (Member, IEEE) was born in Chiba, Japan, in 1987. He received the B.S., M.S., and Ph.D. degrees in electrical engineering from Nihon University, Tokyo, Japan, in 2009, 2011, and 2014, respectively. He was a Research Fellow of the Japan Society for the Promotion of Science (JSPS), in 2013. From 2014 to 2019, he was at the Wireless System Laboratory, Research and Development Center, Toshiba Corporation, as a Research Scientist. In 2019, he joined the Department of Electrical Engineering, College of Science and Technology, Nihon University, where he is currently an Assistant Professor. His research interests include small antennas, tunable antennas, RFID, and fast solvers. He is a member of the IEICE. He received the URSI GASS Young Scientist Award, in 2021.

SHINICHIRO OHNUKI (Member, IEEE) was born in Tokyo, in 1968. He received the B.S., M.S., and Ph.D. degrees in electrical engineering from Nihon University, Tokyo, Japan, in 1991, 1993, and 2000, respectively.

From 2000 to 2004, he was at the Electromagnetics Laboratory and the Center for Computational Electromagnetics, Department of Electrical and Computer Engineering, University of Illinois at Urbana–Champaign, as a Postdoctoral Research Associate and a Visiting Lecturer, and later in 2012, as a Visiting Associate Professor. He joined the Department of Electrical Engineering, College of Science and Technology, Nihon University, in 2004, where he is currently a Professor. His research interests include computational electromagnetics and multiphysics simulation. He was a recipient of the Research Fellowship Award from the Kajima Foundation Tokyo, in 2000. He was a co-recipient of the Best Paper Award from the Magnetic Society of Japan, in 2013; the Technical Development Award from the Institute of Electrical Engineers of Japan, in 2014; and the recipient of the Electronics Society Award from the Institute of Electronics, Information and Communication Engineers, in 2020. He is currently an Editorial Board of Progress in electromagnetics research, since 2017, and an Editorial Advisory Board of Wiley's *International Journal of Numerical Modeling: Electronic Networks, Devices, and Fields*, since 2020. He served as an Associate Editor for the IEEE JOURNAL ON MULTISCALE AND MULTIPHYSICS COMPUTATIONAL TECHNIQUES (2018–2020) and a Secretary for URSI Committee Japan and URSI Commission B (2017–2020).